


Complexities of Lighting Measurement and Calculation

Elena Serea , Codrin Donciu and Marinel Costel Temneanu

Faculty of Electrical Engineering, “Gheorghe Asachi” Technical University of Iași, 700050 Iași, Romania; cdonciu@tuiasi.ro (C.D.); mtemnean@tuiasi.ro (M.C.T.)

* Correspondence: edanila@tuiasi.ro; Tel.: +40-740-481-758

Abstract

Lighting measurements and calculation is an old and widespread process, evolving with the variety of technologies that use light or operate efficiently depending on the natural or artificial light conditions in the ambient environment. The complexity of human activities gives rise to different techniques and approaches to lighting effect analysis, and this paper aims to clarify which type of units, photometric or radiometric, are appropriate, and which light measurement and calculation techniques are optimal for evaluating the environmental microclimate intended for an activity. Quantitative lighting analysis is common and accessible through the measuring devices, calculation formulas, and simulation software available. In contrast, qualitative analysis remains less prevalent, partly due to its complexity and the need to consider human perception as a central component in assessing lighting impact, as emphasized by the human-centric lighting paradigm. Current evaluation frameworks distinguish between the quantitative and qualitative approaches, with actinic calculations addressing biologically relevant aspects of lighting in specific environmental contexts.

Keywords: photometry; radiometry; spectrum; actinic; lighting standard



Academic Editor: Steve Vanlanduit

Received: 30 April 2025

Revised: 7 October 2025

Accepted: 9 October 2025

Published: 13 October 2025

Citation: Serea, E.; Donciu, C.; Temneanu, M.C. Complexities of Lighting Measurement and Calculation. *Metrology* **2025**, *5*, 61. <https://doi.org/10.3390/metrology5040061>

Copyright: © 2025 by the authors. Licensee MDPI, Basel, Switzerland. This article is an open access article distributed under the terms and conditions of the Creative Commons Attribution (CC BY) license (<https://creativecommons.org/licenses/by/4.0/>).

1. Introduction

The common perception of light is that in its natural matter is an infinite regular resource and in its artificial matter is an asset of an installation, contributing alike to our understanding of objects, space, and surroundings. This perception arises from the fact that light, indispensable to any human activity, is always evaluated by the effect it has on the eye, on the ecosystem, and on specially dedicated sensors/collectors.

From a physical point of view, light is more than a visual sensation. It is a complex notion that has intrigued people since ancient times. The first known theories on the nature of light belonged to the ancient Greeks. Pythagoras believed that light was generated by the eye of the observer and propagated in a straight line, while Epicurus believed that on the contrary, light was generated by various objects and then reached the eye of the observer [1]. The Arabs took over the ideas of the Greeks and developed geometric methods that explained quite well how light propagated through all kinds of optical systems such as mirrors, lenses, prisms. The Arabs were also the first to study optical phenomena such as eclipses and rainbows [2].

Ole (Christensen) Rømer, in 1676, published in *Journal des savants* a work explaining an incipient calculus on the value of the speed of light, stating that light takes 22 min to travel a distance equal to the diameter of the Earth’s orbit. The diameter of the Earth’s orbit was not precisely known, but he proved that the speed of light is finite [3]. In 1690, Dutch physicist and mathematician Christiaan Huygens wrote the first *Treatise on Light* [4], stating that light

propagates as a kind of vibration through a pervasive medium he termed the *ether*, which was assumed to fill all space. According to Huygens, light travels through this medium until it interacts with objects, then it reaches the human eye, determining vision [5]. In 1704, its contemporary Isaac Newton discovered that light is actually composed of rays of different colors, a phenomenon known today as the dispersion of light. In a diagram named *Monochord Spectre*, he combined the diatonic scale on a monochord with the spectrum of a prism [6]. Here, the corresponding ratios of string length are indicated and the related spectral colors, in inverse order as have been taken from the prismatic spectrum, are correlated with frequencies of sound and light [7]. Starting from this, Newton considered that light would be made up of small *corpuscles* (term introduced for the first time) of different sizes and properties, a kind of small colored balls, which move very, very quickly in such a way that the eye cannot perceive them. This idea was in contrast to the earlier Christiaan Huygens' wave theory of light. Newton's corpuscular theory suggested that light particles behaved in ways similar to the particles of matter, such as moving in straight lines, reflecting, and refracting. Newton actually elaborated the first corpuscular theory about the nature of light [8]. In the same treatise, he defined the first photometric notions: the incident angle, the angle of reflection, and refraction as we still use them in optics today. Around 227 years later, Einstein would praise Newton's discoveries, highlighting their impact on the development of optical science and color theory [9].

In 1890, the Scottish physicist James Clerk Maxwell described light as a particular case of wave, namely the electromagnetic wave, which we know to be composed of an electric and magnetic field that are generated and propagated together [10]. The electromagnetic wave does not need a support medium in which to propagate, propagating even in a vacuum. Maxwell described light as a transverse, not a longitudinal wave, meaning that the oscillations of the electric and magnetic fields are perpendicular to the direction in which the wave is traveling [11]. Electromagnetic waves differ from each other by their wavelength. Maxwell did not explicitly state the light's wavelengths detailed on colors, but his equations showed that light is just one portion of the broader electromagnetic spectrum. One of the most significant outcomes of his theory was the realization that electromagnetic waves, including light, propagate through a vacuum at a finite speed. This speed is governed by two fundamental physical constants: the permittivity $\epsilon_0 = 8.854187 \times 10^{-12}$ F/m and the permeability of free space $\mu_0 = 1.256637 \times 10^{-6}$ N/A². Permittivity characterizes how an electric field influences and is influenced by a vacuum, while permeability relates to the behavior of magnetic fields in the same medium. These constants define how space itself resists the formation of electric and magnetic fields, and thus determine how quickly electromagnetic waves can travel. This relationship is expressed as follows:

$$c = 1/(\sqrt{\epsilon_0 \times \mu_0}) \quad (1)$$

which is 299,792.456 m/s, approximately 3×10^8 m/s [12].

Only a small part of electromagnetic waves can be perceived by the human eye; we call them light or visible radiation. Their wavelength was not directly measured by Maxwell, but based on its equation and following advances in spectroscopy and precision optics during the 19th and 20th centuries, visible radiation ranged between 380 nm and 750 nm.

In 1905, Albert Einstein brought back into discussion the nature of light, showing that certain physical phenomena such as the photoelectric effect cannot be explained unless it is admitted that, in certain situations, light behaves as a group of particles with extremely special properties (later called photons). Based on the early concept of Max Planck that the microscopic oscillators (atoms) emit and absorb the electromagnetic light in a discontinued manner, in portions and finite packets [1], Einstein stated that light consisted of discrete packets of energy, which he called *quanta*. According to this theory,

the energy E of each quantum of light is proportional only to its frequency ν , according to the following equation:

$$E = h \times \nu \quad (2)$$

where $h = 6.626176 \times 10^{-34} \text{ J}\cdot\text{s}$ is Planck constant [13].

Few years later, Louis de Broglie in his PhD thesis formulated the generality of wave-particle duality concept [14], which implicitly applies to photons, pointing that they can exhibit properties of both waves (like interference and diffraction) and particles (like discrete energy packets) [15].

Planck's groundwork for quantum theory, continued by Einstein's explanation of the photoelectric effect and the predictions of the pilot-wave theory of de Broglie [16], laid the foundations on the notion of photon, revealing a better holistic understanding of the nature of light.

2. From Candlelight to Candela

All the early studies of light converge in that light intensity could be measured. The first attempts on standardizing light measurement began in the 18th century. Early units of light intensity were often based on natural sources, such as the brightness of sunlight or moonlight, or on specific artificial light sources.

In 1830, Pecllet introduced the standard for the stearin “Star” candle in France, refining the earlier Monnier candle (1810), which had a diameter of 20 mm and a flame height of 52.2 mm. This standard was defined as 0.136 of the Carcel lamp's output, an early oil lamp invented by Léon-Philippe Carcel, which featured a clockwork mechanism for regulating oil flow and achieving a more consistent light output. However, this reliance on a specific lamp's output limits the flexibility of the standard, as it ties light intensity to a particular design. Meanwhile, in Germany, two candles were standardized: the “Vereinskerze” (20 mm diameter, 50 mm flame height) in 1868, used for general lighting purposes, and the Munich Candle, a tallow-based candle with variable dimensions (20.5–23 mm diameter, 56 mm flame height), employed to regulate gas lighting systems. These standards illustrate the regional variations in light intensity measurement, yet both tied to specific, locally used lighting systems [17]. In Britain, the Metropolitan Gas Act of 1860 formalized the “British Parliamentary Candle,” made from sperm whale oil, with a 20.5 mm diameter and a burn rate of 7.8 g per hour. While these standards helped regulate gas lighting, their reliance on a specific material and burn rate limits their broader applicability. Table 1 provides a comparative overview of these historical standards.

Table 1. Parameters of the first standardized candles [18,19].

Candle	Height of Flame [mm]	Hourly Consumption [g]	Value in Carcels
French	52.2	12	0.136
British	46	7.8	0.120
German Veriens	50	7.5	0.134
German Munich	55	10.4	0.153

Thus, based on the brightness of a standardized candle, the term *candle-power* was firstly introduced to describe the luminous intensity of a light source, essentially referring to how bright the light emitted from a source appears to be in a given direction. Photometric etalons began to appear in the form of light sources that provided known and reproducible levels of luminous intensity. These could be used to calibrate photometers, to measure and compare the brightness of various light sources, including gas lamps. Given the necessity of a precise light etalon, in 1909, the International Candle was introduced—through an

international agreement during the International Conference on the Meter—as the standard reference for luminous intensity [20]. A wider acceptance of the International Candle took place in 1921, when the International Commission on Illumination (CIE) adopted the carbon-filament incandescent lamp. This more advanced approach compared to the standard fuel-based candles, and oil lamps had defined characteristics, including a specific filament material, size, and operating voltage, but had the limitations of filament rapid aging [21]. It became the new standardized light source for photometric measurements, and its consistent output made it an ideal standard for photometric measurements at the time.

As a measurement, the candle power and, lately, the International Candle were widely used [22] until the International System of Units (SI) introduced the candela as the official unit of luminous intensity in 1948 [23]. Its subsequent evolution, presented in Table 2, is due to immediate evolution of photometry in terms of optical radiation power measurement. This advancement has enabled new approaches in photometry, redefining the candela in addition to high-temperature Planck radiators [24]. The key advantage of using a blackbody source was the ability to compute its spectral radiance directly through Planck’s law. This law mathematically describes how the intensity of electromagnetic radiation emitted by a black body depends on its temperature and wavelength, forming the theoretical basis for earlier photometric standards. The spectral radiance is expressed as

$$L_{e,\lambda}(T, \lambda) = (c_1 / \pi \times \Omega_0) \times [n^2 \lambda_0^5 (\exp(c^2 / n \times \lambda_0 \times T) - 1)]^{-1} \quad (3)$$

where Ω_0 is the solid angle, n is the refractive index, λ_0 is the vacuum wavelength, T is the temperature. The constants $c_1 = 2\pi h c^2 = 3.7418 \times 10^{-16} \text{ W} \cdot \text{m}^2$ and $c_2 = h \times c / k = 0.01439 \text{ m} \cdot \text{K}$ are derived from Planck’s constant h , Boltzmann’s constant k , and the speed of light c .

Table 2. Evolution of the notion of candela as a light measurement (after [21]).

Notion	Adopted by	Year	Definition
Candle-power	Great Britain	1860	The light produced in a specific direction by a pure Spermaceti Candle weighing 1/6 lb and burning at a rate of 120 grains per hour.
International candle	Laboratoire Central de l’Electricité (Paris)	1909	The light output of a <i>Carcel burner</i> consuming 42 g/h of rapeseed oil.
International candle	CIE	1921	The luminous intensity of a light source in terms of a standardized carbon filament incandescent lamp.
The candela	CIPM *, CIE	1948	The luminous intensity of a light source that radiated 1/683 watt per steradian at a wavelength of 555 nm (green light), which is the peak sensitivity of the human eye.
Candela	CGPM **	1967	The luminous intensity, in the perpendicular direction, of a surface of 1/600,000 m ² of a blackbody at the temperature of freezing platinum under a pressure of 101,325 N/m ² (based on <i>blackbody radiation</i>).
Candela	CGPM	1979	The luminous intensity, in a given direction, of a source that emits monochromatic radiation of frequency $540 \times 10^{12} \text{ Hz}$ and that has a radiant intensity in that direction of 1/683 W per steradian (based on <i>radiant intensity of a monochromatic radiation</i>).

Table 2. Cont.

Notion	Adopted by	Year	Definition
Candela	CGPM	2019	The luminous intensity in a given direction. It is defined by taking the fixed numerical value of the luminous efficacy of monochromatic radiation of frequency 540×10^{12} Hz, K_{cd} to be 683, when expressed in the unit [lm/W], which is equal to [cd·sr/W], or [cd·sr·kg ⁻¹ ·m ⁻² ·s ³], where the kilogram, meter, and second are defined in terms of h , c , and $\Delta\nu_{Cs}$ (based on a defining constant).

* International Committee for Weights and Measures. ** General Conference on Weights and Measures.

The current definition of the candela, adopted in 1979, specifies luminous intensity at a single optical frequency.

The 2019 redefinition of the candela no longer references a light source, addressing common misinterpretations in earlier definitions. It also omits an explicit definition of the luminous intensity quantity itself, allowing any suitable metrological principle to be used for its realization, provided the fixed constant used to scale the unit is applied. The extension “in a given direction” from the first part of the definition is redundant, because the formula of luminous intensity involves the luminous flux and the solid angle, already establishing that luminous intensity is a directional quantity [25].

The need for an international metrology authority emerged nearly a century ago. In 1927, Einstein, Marie Curie, and Hendrik Lorentz advocated for its creation in a report to the International Committee on Intellectual Cooperation. This led to the establishment of an international bureau in 1955, initially focused on standardizing length and time using light-based references. Einstein’s use of light rays to measure the distance of a moving body, in his 1905 theory of special relativity, indirectly laid the groundwork for electromagnetic standards, influencing the 1960 adoption of the international length standard by the International Legal Metrology Organization [15].

3. Photometry Instruments

3.1. Etalons in Light Measurement

The working principle of an etalon is based on interference: light enters the cavity between two reflective surfaces, and multiple reflections occur. Further, some rays exit the cavity after a few reflections, and interference effects result in specific transmission peaks based on the wavelength of light and the distance between the reflective surfaces. Thus, the etalon serves as a precise spectral filter, selectively transmitting certain wavelengths while attenuating others. The transmitted wavelengths are determined by the condition for constructive interference, which depends on the optical path length between the reflective surfaces. By adjusting the spacing between these surfaces or modifying the refractive index of the medium within the cavity, the transmitted wavelengths can be finely tuned.

Emerging from this phenomenon, Fabry-Pérot interferometer was built in 1899, based on which, lately, interferometric sensors were developed [26]. As presented in Figure 1, the reflected rays interfere with each other to produce sharp fringes in the transmitted field. After focusing by lens, the interference fringes result in a set of concentric circles. To achieve bright circular fringes, the path length difference between two adjacent rays must match the condition:

$$2d \times \cos(\theta) = m \times \lambda/\mu \quad (4)$$

where d is the distance between the two reflective surfaces, θ is the incident angle of the light of λ wavelength, and μ is the refractive index of the propagation medium. The interference

order m is an integer which describes the number of wavelengths fitting into the optical path difference between successive reflections in an etalon, indicating the constructive interference condition where light of wavelength λ can resonate within the cavity. Higher values of m correspond to higher-order interference fringes, meaning the light undergoes more reflections before exiting. In other words, the spacing between fringes is determined by m , with larger values leading to narrower spectral peaks in transmission. Etalons' capacity to provide narrowband spectral selection enhances measurement accuracy and system performance.

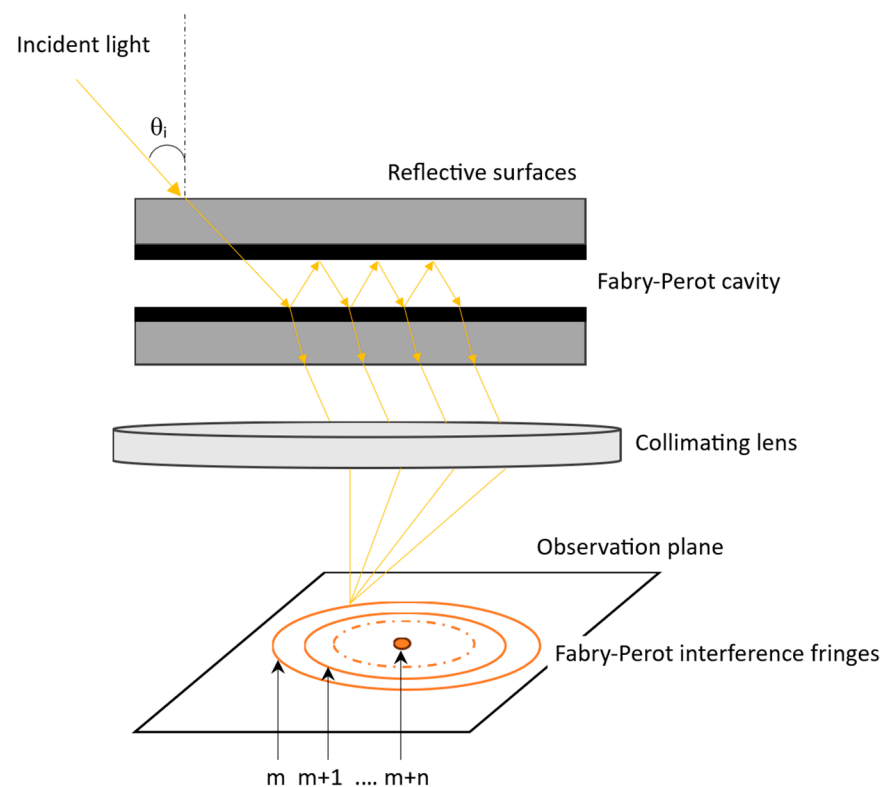


Figure 1. Schematic working principle of a Fabry–Pérot interferometer. Redrawn and adapted after [27].

In light measurement, etalons serve distinct roles depending on spectral resolution requirements and application contexts. The air-spaced etalon, consisting of two parallel mirrors separated by a controllable air gap, enables precise and tunable spectral filtering. The Fizeau etalon, which uses closely spaced, slightly tilted reflective surfaces, generates high-contrast interference fringes and is used for its stability in wavelength discrimination. The solid etalon, fabricated from a single transparent medium with reflective coatings, provides fixed spectral resolution, with structural robustness and simplicity.

Other types, such as the Gires–Tournois etalon (which uses asymmetric mirrors for phase control and dispersion compensation [28]), the confocal etalon (which uses curved mirrors to improve alignment and resolution [29]), and tunable etalons (which adjust mirror spacing for flexible spectral filtering [30]), are more common in laser systems and optical communication. These devices offer high precision but are generally too complex or specialized for routine light measurement tasks in metrology. As a result, their use in standard lighting applications is limited, despite their technical capabilities.

3.2. Instruments for Quantitative and Qualitative Lighting Analysis

The proper usage of measurement instruments in lighting analysis involves first establishing which type of analysis, quantitative or qualitative, has to be developed. Depending on this, key lighting parameters to be measured will be set and the instrumentation suitable for them will be chosen. Instruments must be properly calibrated according to manufacturer specifications and standards and, if required, dark calibration must be performed.

The first scientific attestation of the achievement of a photometer was published in 1760 by Pierre Bouguer. The instrument compared the brightness of two light sources, a standard lamp and a test lamp, whose distance from the screen (D_t and D_s) was modified until the comparison screen achieved the equal perceived brightness on each side (Figure 2a). Concomitant, Johann Heinrich Lambert developed a photometer (Figure 2b) intended on quantifying light attenuation through a medium. The same two sources cast two shadows from the rods on the screen, and the observer equalized the two intensities visually. Its first practical application was in 1792 in a military house in Munich, when Benjamin Thompson, also known as Count Rumford, compared different candles and gas lamps to quantify their efficiency [31]. Before Rumford, photometric comparisons were mostly qualitative (subjective observations). His method introduced a more practical, repeatable, and easy-to-use approach for measuring light intensity. Both photometers were designed based on the principles of light attenuation and intensity comparison, leading to the development of Bouguer's Law (Equation (5)) and later the Beer-Lambert Law (Equation (6)).

$$I = I_0 \times e^{-\alpha x} \quad (5)$$

$$I = I_0 \times e^{-\varepsilon \cdot c \cdot x} \quad (6)$$

where I is the transmitted intensity, I_0 is the initial intensity, α is the absorption coefficient, x is the path length, ε is the molar absorptivity or the extinction coefficient, and c is the concentration of the absorbing species in the medium, not the concentration of the medium itself.

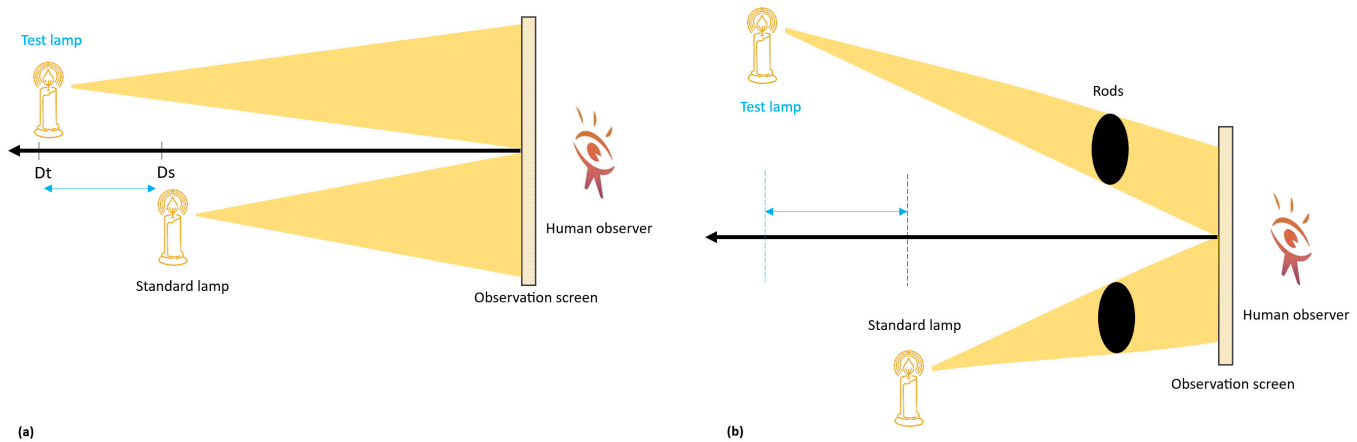


Figure 2. Comparison of Bouguer's (a) and Lambert's (b) Photometers.

Modern photometers available today incorporate advanced sensors with photopic filters, automation, and AI-based analysis software which improve precision and reduce operator dependency [32]. However, despite these technological advancements, the instruments remain sensitive to spectral mismatch, particularly with LED sources, highlighting a trade-off between automation and measurement accuracy. High-end photometers feature wide dynamic ranges, allowing measurements from low-light conditions (~ 0.01 lx) to high-intensity sources ($> 200,000$ lx), and use low-noise amplifiers and digital signal processing (DSP) to enhance sensitivity and stability. Yet, their cost and complexity may limit routine

deployment in standard lighting audits, emphasizing the need to balance performance and application context. They operate based on radiometric, photometric, and spectroscopic principles, depending on their application and their basis equations are the inverse square law (7), luminance definition (8), and Beer-Lambert law (6), integrating sphere luminous flux Equation (9) [33],

$$E = I_{\alpha} \times \cos\theta / d^2 \quad (7)$$

$$L = I_{\alpha} / (A \times \cos\alpha) \quad (8)$$

$$\Phi = L_s \cdot A_d \cdot \Omega \quad (9)$$

where α is the angle of emission, L_s is the sphere surface radiance, A_d is the detector active area, and $\Omega = \pi \times \sin^2\theta$ is the projected solid angle of the detector's field of view.

Lighting measurement and analysis involves both **quantitative** and **qualitative** aspects. Understanding the distinction ensures accurate evaluations and appropriate solutions for various lighting needs, from small projects [34] to large complex architectural ones [35]. Quantitative measurements refer to numerical values that describe the physical properties of light, while qualitative measurements focus on the subjective perception of light. One particular note on luminance has to be made in this context: if luminance is considered as the value in cd/m^2 of brightness perceived from a surface, it is a quantitative parameter; if it is referred to as the perceived ambient lighting comfort (whether the space feels appropriately lit), luminance is a qualitative parameter. A brief overview of the category lighting measuring equipment is given in Table 3. Quantitative instruments ensure precision, compliance, and performance optimization in lighting systems, and qualitative instruments assess human perception, comfort, and aesthetic impact in lighting design; so, both are essential in effective lighting analysis, providing a comprehensive approach.

Table 3. Comparison of measurement instruments for quantitative and qualitative lighting analysis.

Instrument	Output Parameter	Basis Equation	Mathematical Considerations
Lux meter	Illuminance (lux)	$E = \Phi / A$	As it approximates human eye's response using filters, spectral correction factors based on the photopic curve must be applied : $S_{corr} = \frac{\int S(\lambda)V(\lambda)d\lambda}{\int V(\lambda)d\lambda}$ [36].
Spectroradiometer	Spectral power distribution (W/m^2)	$S(\lambda) = d\Phi / d\lambda$	As it uses Fabry – Péro interferometers, airy function has to be used for multiple internal reflections correction : $T = \frac{1}{1 + F \sin^2(\frac{\theta}{2})}$ [37].
Quantitative	Integrating sphere	Total luminous flux (lm)	As it assumes uniform light distribution, errors arise from wall reflectance, port losses or baffle placement. A general correction can be expressed as follows : $\Phi_{corr}^* = \frac{\Phi_{measured}}{f_b} \cdot \left[1 - \rho \left(1 - \frac{A_p}{A_s} \right) \right]$ (derived from the principles in [33]). f_b is baffle correction factor obtained experimentally by measuring a reference source with and without the baffle (i.e., the ratio of the corresponding detector responses) or by means of ray-tracing simulations, ρ is average sphere wall reflectance, A_p —port area, A_s —total sphere's internal surface area.
	Goniophotometer	Angular light distribution ($^\circ$)	Because the definition of luminous intensity assumes ideal Lambertian emission, real sources that deviate from this distribution require adjustment using the angular distribution function : $I(\alpha) = I_0 \cos^n(\alpha)$ [38]
	Luminance meter	Luminance (cd/m^2)	The standard luminance definition is exact for Lambertian emitters. For non-Lambertian sources, angular corrections are applied: $L(\alpha) = L_0 \cos^n(\alpha)$.

Table 3. Cont.

	Instrument	Output Parameter	Basis Equation	Mathematical Considerations
Qualitative	Luminance distribution meter (with glare evaluation software)	Glare indices (UGR, DGI, fTI, etc.)	$UGR = 8 \log_{10} \left[\frac{0.25}{L_b} \frac{L_s^2 \Omega}{p^2} \right]$	Measurement uncertainty arises mainly from instrument calibration affecting luminance, specifically, background and source luminance (L_b and L_s) distribution capture that influence Ω and environmental conditions (e.g., lens distortion, stray light) that affect the Guth position index p [39].
	Colorimeter	CCT, RGB values, XYZ coordinates	$X, Y, Z(\lambda) = \int S(\lambda) \cdot \overline{X}, \overline{Y}, \overline{Z}(\lambda) d\lambda$	Is based on CIE 1931 XYZ color space account for human color perception, approximating the eye's response to different wavelengths. The obtained values can be further converted into CIE Lab or RGB color spaces for different applications [40].
	Spectroradiometer (with CRI/TM-30 evaluation software)	CRI, TM-30	$\Delta E = \frac{\Delta E}{\sqrt{(L_2 - L_1)^2 + (a_2 - a_1)^2 + (b_2 - b_1)^2}}$	CRI and TM-30 values are calculated from the measured spectral power distribution (SPD) of the light source. Their accuracy depends on the instrument's spectral resolution, calibration, and on the algorithm used for the calculation. As human color perception is non-linear, the color difference (ΔE) equation is used to determine perceptible color differences in various lighting environments [41].
	Hemispherical photography	Light distribution patterns	Image processing algorithms	Distortion and calibration errors often occur, as wide-angle lenses introduce geometric distortions that must be corrected [42].

* Φ_{corr} is the flux after applying geometric and sphere-multiplication corrections—i.e., the best estimate of the lamp's emitted flux under the intended reference geometry.

Even if modern photometers are technically advanced, random and systematic errors can occur. Random errors indicate the precision or repeatability of a measurement and can be minimized by conducting multiple trials. In contrast, systematic errors persist regardless of repeated measurements and must be identified and quantified by the experimenter or system operator. In total luminous flux measurements, the most notable systematic error is the calibration uncertainty associated with the working standard lamp: as most photometers approximate the CIE $V(\lambda)$ curve—the spectral luminous efficiency function for photopic vision, light sources with different spectral distributions but similar perceived brightness may yield the same illuminance measurement. So, achieving a perfect match to the $V(\lambda)$ curve is challenging, often resulting in significant spectral mismatch errors, especially in the blue region. Modern light sources, such as LEDs, often emit strong blue components, leading to inconsistencies between different lux meters. These errors may remain undetected during calibration with incandescent sources, as their smooth spectrum averages out discrepancies [43].

Each photometric instruments have to comply with specific standards such as ISO 17025, [44] required for testing and calibration laboratories and CIE 198-SP2:2018 [45], which defines uncertainty analysis procedures in photometry. Measurement uncertainty is typically classified into contributions from random errors and systematic errors, the latter being non-correctable. A measurement with minimal random error is considered highly precise, indicating good repeatability. Conversely, a measurement with minimal systematic error is considered to have high trueness, reflecting its accuracy in representing the true value (Figure 3). Measurement uncertainty extends beyond instrument calibration and repeatability variations. A comprehensive assessment must consider factors such as environmental conditions, test procedures, operator expertise, and the characteristics of the measured object—each contributing to overall uncertainty. Reducing uncertainty may involve applying corrections based on equipment knowledge and source properties, such as spectral mismatch correction factors, or conducting additional tests [46].

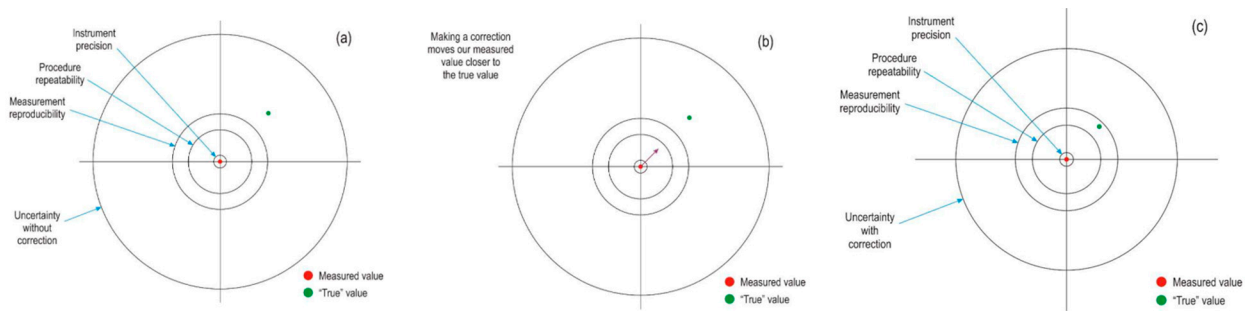


Figure 3. Relationship between accuracy, uncertainty, and correction: (a) measured value, “true” value, and contributions to measurement uncertainty; (b) making a correction to the measurement result; (c) improved situation after making a correction [46].

Since photometric measurements involve multiple uncertainty sources—such as sensor calibration, spectral mismatch, noise, environmental factors, and instrument precision—it is essential to combine these individual contributions into a single value that reflects the overall measurement confidence. This is done using the root-sum-of-squares method, a standard approach in metrology for propagating uncertainty from independent sources [47]. The total combined uncertainty is given by

$$u_{total} = \sqrt{u_{reference}^2 + u_{transfer}^2 + u_{measurement}^2} \quad (10)$$

where $u_{reference}$ accounts for uncertainties from the reference standard, $u_{transfer}$ captures errors introduced during calibration transfer, and $u_{measurement}$ represents the uncertainty in the actual measurement process.

In Table 4, particular emphasis is placed on the relevance of error origins as spectral mismatch, angular deviation, or calibration drift, which critically influence measurement reliability and should be carefully considered in both instrument selection and uncertainty assessment.

Table 4. Comparative analysis of lighting measurement instruments with error sources.

Instrument	Common Application	Primary Error Sources	Limitations
Lux meter	General lighting audits, workspace compliance	Spectral mismatch error ($V(\lambda)$ approximation), cosine error	Inaccurate under non-standard spectra (e.g., LED); angle sensitivity
Spectroradiometer	Light source spectrum characterization, CRI/CCT analysis (product display lighting, architectural lighting)	Stray light, thermal drift, wavelength calibration inaccuracy Reference data inaccuracies, non-linear perception modeling	Requires stable environment and calibration Incorrect perception if using outdated color samples
Integrating sphere	Calibration of photometric instruments, luminous flux measurement, reflectance and transmittance testing	Port losses, non-uniform reflectance, baffle misalignment	Large dimensions, sensitive to geometry, needs correction factors
Goniophotometer	Beam angle distribution, automotive headlamp design	Positioning errors, mechanical backlash, detector alignment	Large dimensions, time-intensive setup
Luminance meter	Display testing, road visibility and safety, brightness uniformity, office lighting, indoor workspaces	Angular error, vignetting, stray light, inconsistent background luminance	Sensitive to measurement distance and viewing geometry. High sensitivity with small changes in environment
Colorimeter	Ambiental lighting design, rapid color checks	Filter drift, limited spectral resolution, ambient light contamination	Low precision compared to spectroradiometers
Hemispherical photography	Solar radiation and daylighting analysis, light distribution and luminance mapping, architectural and horticultural visualizations, lighting simulation and assessment in 3D environments	Lens distortion, exposure miscalibration, sensor vignetting	Requires complex correction algorithms; error-prone under dynamic light

4. Radiometric, Photometric, and Quantum Parameters

As stated by Maxwell, a light wave consists of electric and magnetic fields oscillating perpendicularly to each other, propagating both through matter and through a vacuum. Because light has numerous effects on matter (through absorption, reflection, refraction, transmission, leading to scattering, polarization, photosynthesis, optical tweezing, photoelectric effect, photovoltaic effect, radiation pressure, second harmonic generation, self-focusing, psychological and biophysical effects other than visual), various units are used to quantify light intensity. Light can be described from three complementary perspectives: radiometric, photometric, and quantum, depending on whether it is treated as physical radiation, as perceived luminous sensation, or as a stream of photons. Presenting them in this logical order clarifies how physical energy is converted into visual sensation and, ultimately, into photon-based quantification.

4.1. Radiometric Units

Used for non-visual effects of light, radiometric units characterize electromagnetic radiation in terms of energy. The SI unit for radiant energy (symbol Q) is the Joule. A closely related radiometric quantity is radiant flux (symbol Φ_e), which is radiant energy per unit of time, measured in Watts. Depending on the geometry of the measuring setup, additional radiometric quantities may be introduced, resulting in derived units for measurement results (e.g., radiance [$W/m^2 \text{ sr}$], irradiance [W/m^2], or radiant flux density [W/m^2], often confused with the quantum measure actinic flux [$\mu\text{mol photons}/m^2 \text{ s}^{-1}$]).

4.2. Photometric Units

Used for visual effects of light, photometric units characterize electromagnetic radiation based on the luminous sensation perceived by the human eye. Any photometric quantity (luminous flux, luminance, illuminance, luminous intensity, generally denoted by X) can be calculated from the associated spectral radiometric quantity ($X(\lambda)$) with the formula:

$$X = K_m \int_{\lambda_1}^{\lambda_2} X(\lambda) \cdot V(\lambda) d\lambda \text{ or } X = K_m \sum X(\lambda) \cdot V(\lambda) \cdot \Delta\lambda \quad (11)$$

where

- $V(\lambda)$ is the relative spectral luminous efficacy function (defined by the CIE spectral sensitivity function), which has a maximum value of 1 corresponding to the wavelength of 555 nm for daylight (photopic) vision and to 507 nm for night (scotopic) vision, $V'(\lambda)$ —Figure 4. The values of $V(\lambda)$ for visible wavelengths were statistically established by CIE (International Commission on Illumination) for the average eye, first for a standard photometric observer with a viewing angle of 2 degrees (in 1932), then for a 10-degree observer (1964). Lighting researchers and practitioners prefer to use the original CIE spectral luminous efficacy function $V_2(\lambda)$ (2-degree standard observer) [48], because it describes the cone vision within the fovea (cones being the color receptors of the eye and having the fastest response kinetics to altered lighting—20 ms [49]). For calculation, reference values of $V(\lambda)$, $V'(\lambda)$ and conversion factors are given in Table 5.

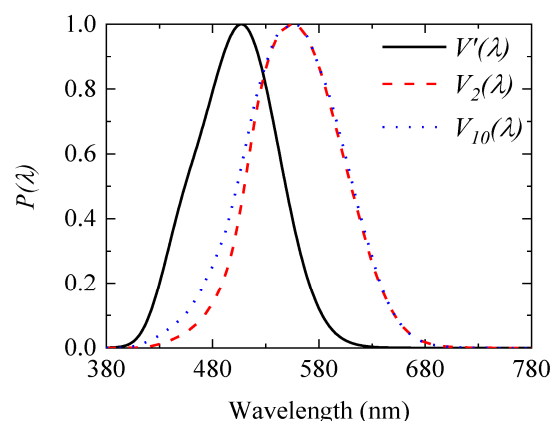


Figure 4. Spectral sensitivity curves of the human eye [50].

Table 5. Spectral luminous efficacy for photopic and scotopic vision and corresponding conversion factors (Values are rounded to six decimals for readability. The rounding introduces an absolute uncertainty of $\pm 5 \times 10^{-7}$ in the last digit. Photopic and scotopic luminous efficacy values are nominal; for high-precision metrological applications, readers should refer to the full-precision 13-decimal source data from CIE 018:2019 [51,52]. Photopic and scotopic conversion factors are calculated based on these rounded $V(\lambda)$ and $V'(\lambda)$ values).

Wavelength λ [nm]	Spectral Luminous Efficacy for Photopic Vision $V(\lambda)$	Photopic Conversion Factor [lm/W]	Spectral Luminous Efficacy for Scotopic Vision $V'(\lambda)$	Scotopic Conversion Factor [lm/W]
380	0.000039	0.027	0.000589	1.001
390	0.000120	0.082	0.002209	3.755
400	0.000396	0.270	0.009290	15.793
410	0.001210	0.826	0.034840	59.228
420	0.004000	2.732	0.096600	164.220
430	0.011600	7.923	0.199800	339.660
440	0.023000	15.709	0.328100	557.770
450	0.038000	25.954	0.455000	773.500
460	0.060000	40.980	0.567000	963.900
470	0.090980	62.139	0.676000	1149.200
480	0.139020	94.951	0.793000	1348.100
490	0.208020	142.078	0.904000	1536.800
500	0.323000	220.609	0.982000	1669.400
507	0.444310	303.464	1.000000	1700.000
510	0.503000	343.549	0.997000	1694.900
520	0.710000	484.930	0.935000	1589.500
530	0.862000	588.746	0.811000	1378.700
540	0.954000	651.582	0.655000	1105.000
550	0.994950	679.551	0.481000	817.700
555	1.000000	683.000	0.402000	683.000
560	0.995000	679.585	0.328800	558.960
570	0.952000	650.216	0.207600	352.920
580	0.870000	594.210	0.121200	206.040
590	0.757000	517.031	0.065500	111.350
600	0.631000	430.973	0.033150	56.355
610	0.503000	343.549	0.015930	27.081
620	0.381000	260.223	0.007370	12.529
630	0.265000	180.995	0.003335	5.670
640	0.175000	119.525	0.001497	2.545
650	0.107000	73.081	0.000677	1.151
660	0.061000	41.663	0.000313	0.532
670	0.032000	21.856	0.000148	0.252
680	0.017000	11.611	0.000072	0.122
690	0.008210	5.607	0.000035	0.060
700	0.004102	2.802	0.000018	0.030

- K_m is the maximum luminous efficacy of radiation, equal to 683 lm/W for photopic vision (at 555 nm) and 1700 lm/W for scotopic vision (at 507 nm). However, the difference between these two values of K_m does not reflect the relative magnitude of the luminous response (or perceived brightness) for the two types of vision. As seen from Table 5, they only reflect the definition of light levels and the normalization convention of the two functions at the peak wavelengths. This standard value of 683 lm/W for the maximum luminous efficacy of radiant power was formally introduced in 1979 during the 16th General Conference on Weights and Measures (see Table 2), when the photometric quantities in the International System of Units (SI) were redefined in terms of physical constants. There marked a key moment in the integration of photometric and radiometric systems, ensuring consistency in the science and engineering of light.

Normally, only discrete values for $X(\lambda)$ and $V(\lambda)$ are known, and the summation in Equation (13) is performed over intervals of 1, 5, or 10 nm. In this equation, additivity is assumed by definition and yields good results; however, for higher precision, the sum must be weighted by the sample value. Equation (13) outlines three fundamental principles of the current photometric systems:

- The use of spectral weighing functions with radiometric quantities.
- The law of arithmetic additivity for photometric quantities.
- The choice and definition of the photometric base unit, including the setting of its magnitude [23].

As a calculation rule, unless specifically mentioned, photometric quantities or units refer to daylight vision.

4.3. Quantum Units

Quantum units express radiation in terms of discrete energy particles—photons or quanta, acknowledging the particle-like nature of light. Each photon carries a finite amount of energy, and therefore, the conversion between radiometric and quantum quantities is inherently wavelength dependent. The energy of a single photon, E as in Equation (2), is determined by its wavelength, λ , linking the continuous wave description of radiation to its discrete quantum representation:

$$E = h \times c / \lambda \quad (12)$$

where h is Planck's constant, and c is the speed of light in a vacuum (speed reduces as light passes through a medium and is inversely proportional to the refractive index of the medium).

To determine the number of quanta (photons) associated with the total radiant energy of a source E_{total} , the following formula is used:

$$q = E_{total} / E = E_{total} \times \lambda / h \times c \approx 5.043 \times 10^{15} \times E \times \lambda \quad (13)$$

For the energy quantities associated with polychromatic light sources, precise conversion between radiometric, quantum and photometric units is only possible if the spectral distribution of the light source is known in advance or can be measured. This requirement arises because each system of units weights the spectral components differently—by energy, by human visual sensitivity or by photon count. Table 6 renders a correspondence between these three systems of quantities.

Table 6. Related quantities describing the light visual and non-visual effect.

Radiometric (Energetic) Units		Photometric Units		Quantum Units	
Quantity	Symbol and SI Unit	Quantity	Symbol and SI Unit	Quantity	Symbol and SI Unit
Radiant energy	Q_e [J]	Luminous energy	Q_l [lm·s]	Photon energy	E [J]
Radiant flux	Φ_e [W]	Luminous flux	Φ [lm]	Photon flux	Q [photons/s]
Radiant intensity	I_e [W/sr]	Luminous intensity	I [cd]	-	-
Radiance	L_e [W/m ² ·sr]	Luminance	L [cd/m ²]	-	-
Irradiance or radiant flux density	E_e [W/m ²]	Illuminance or luminous flux density	E [lx]	Photon irradiance	E_q [photons/(m ² ·s)]

4.4. Example of Conversion from Radiometric to Photometric Quantities

The relationships summarized in Table 6 enable practical conversion between energetic and perceptual quantities, as illustrated below for the common case of converting radiometric data into photometric values.

As example, if using a spectrophotometer to capture the action spectrum of a natural or artificial light source, its luminous flux can be calculated. The flux can be incident on a surface from any direction (Figure 5a) or can be reflected or emitted by the surface (Figure 5b). In the first case, the usual measure is the flux density on the surface (or irradiance), while in the second case, the usual measure is radiant flux density (or emittance).

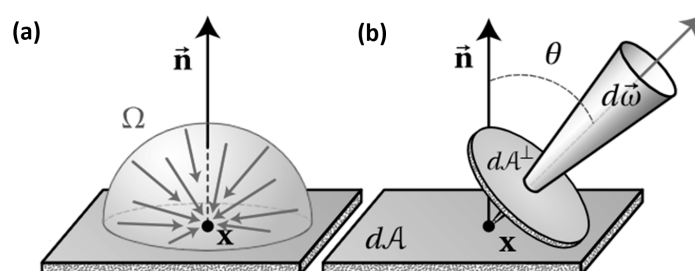


Figure 5. (a) Radiant flux reaching a surface (irradiance); (b) flux leaving a surface due to emission or reflection (emittance) [53].

The flux that reaches the surface (Φ_e) is calculated from the formula of the irradiance definition:

$$E_e = d\Phi_e/dA \text{ [W/m}^2\text{]} \quad (14)$$

Respectively, the flux corresponding to a specific wavelength, $\phi_{e(\lambda)}$, results from the spectral irradiance formula:

$$E_e(\lambda) = d\Phi_e(\lambda)/dA \cdot d\lambda \text{ [W/m}^2 \cdot \text{nm]} \quad (15)$$

Based on the measured spectral irradiance $E_e(\lambda)$ —from the action spectrum of the light source, the corresponding radiant flux $\Phi_e(\lambda)$ for certain wavelengths (from 10 to 10 nm as example) can be extracted from Equation (15). The total luminous flux of a light source Φ_l can be determined with the formula derived from (11):

$$\Phi_l = 683 \cdot \sum \Phi_e(\lambda) \cdot V(\lambda) \cdot \Delta\lambda \text{ [lm]} \quad (16)$$

4.5. Radiative Transfer and Light Propagation in Media

The quantitative relationships discussed in the previous subsections form the basis for modeling light propagation in real media. In lighting calculations, some equations become particularly complex due to the need to integrate variables over space, wavelength or angular distributions. Among these, the radiative transfer equation (RTE) is the most

complicated, as shown in Equation (17), stated for a monochromatic radiation. It is fundamental in describing the behavior of light as it interacts with a medium (losing energy by absorption, gaining energy by emission, and redistributing energy by scattering) and how the existing physical fields are transformed according to the physiognomy of fixtures [54].

$$\frac{1}{c} \cdot \frac{dI(r, \Omega, \lambda)}{dt} = -\kappa(r, \lambda) \cdot I(r, \Omega, \lambda) + j(r, \Omega, \lambda) + \int_{\Omega_1} P(\Omega, \Omega_1, \lambda) I(r, \Omega_1, \lambda) d\Omega_1 \quad (17)$$

$I(r, \Omega, \lambda)$ is the specific intensity of light at position r , traveling in direction Ω , at the wavelength λ ;

κ is the absorption coefficient, representing the light/radiation absorbed per unit length of the medium or the attenuation of light due to absorption by the medium;

j is the emission coefficient, representing the light/radiation emitted by the medium per unit volume, per unit frequency;

$\int_{\Omega_1} P(\Omega, \Omega_1, \lambda) I(r, \Omega_1, \lambda) d\Omega_1$ represents the light scattered from all directions Ω_1 , where $P(\Omega, \Omega_1, \lambda)$ is the phase function, describing the probability of scattering from direction Ω_1 to Ω .

For polychromatic radiations, Equation (17) has to be integrated over all frequencies, and the frequency-integrated variables replace their monochromatic counterparts:

$$\frac{1}{c} \cdot \frac{dI}{dt} = -\kappa \cdot I + j + \int_{\Omega_1} P(\Omega, \Omega_1) I(\Omega_1) d\Omega_1 \quad (18)$$

The scattering coefficient and the phase function remain dependent on wavelength, so the full integration over all frequencies is complex. Real-world problems often involve complex boundaries, such as interfaces between different materials, making analytical solutions impossible. Thus, solving RTE requires numerical methods, specific to the practical application (like discrete ordinate in engineering [55], Monte Carlo and ray tracing in astrophysics [56,57], spherical harmonics in optics [58], band models in climatology [59]).

As an example, if applying RTE for a polychromatic radiation in a cloudy atmosphere, few approximations have to be considered: knowing that clouds contain water droplets and aerosols, which scatter and absorb light differently across the visible and near-infrared spectrum, wavelength-dependent effects must be approximated for several spectral bands (e.g., blue 450 nm strong scattering, green 550 nm moderate scattering, red 650 nm moderate absorption, near-infrared 850 nm high absorption, infrared 1050 nm stronger absorption). If the medium is approximated to 1D plane-parallel (Figure 6), the steady state RTE is

$$\mu \frac{dI_\lambda}{dz} = -(k_\lambda + \sigma_\lambda) \cdot I_\lambda + \frac{\sigma_\lambda}{4\pi} \int_{4\pi} P(\Omega, \Omega_1) \cdot I_\lambda(\Omega_1) d\Omega_1 \quad (19)$$

where μ is $\cos(\theta)$, $\frac{dI_\lambda}{dz}$ is the radiance gradient, σ_λ is the scattering coefficient, and $(k_\lambda + \sigma_\lambda)$ is the extinction coefficient, representing the total energy removed along the path.

Finding solutions to this equation requires other approximations, besides the discrete wavelength approach. In the literature are presented several specific methods (Table 7), each providing good results in a specific application, with the implicit limitations.

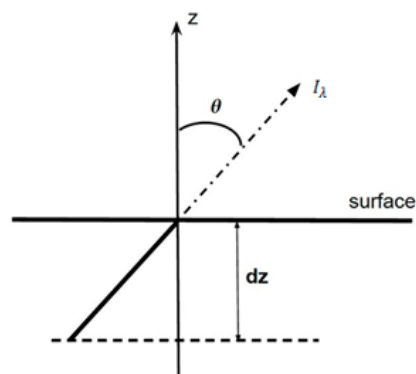


Figure 6. One-dimensional plane-parallel representation for radiative transfer of light emitted in atmosphere (after [60]).

Table 7. Common approximations for solving the radiative transfer equation (RTE) in polychromatic media.

Method	Mathematical Approach	Specific Applications	Advantages	Limitations
Two-Stream Approximation	Reduces angular dependence to two directions (upward and downward)	Climate models, remote sensing	Captures bulk radiation behavior	Poor accuracy for highly anisotropic scattering
Diffusion Approximation	Treats radiation as diffusive transport	Cloud physics, biomedical optics	Converts RTE into a simpler diffusion equation	Inaccurate for optically thin layers
Rayleigh & Mie Scattering Approximations	Approximates scattering behavior for different particle sizes (Rayleigh and Mie—small and large particles)	Cloud optics, aerosol modeling, atmospheric physics	Captures dominant scattering effects	Rayleigh fails for large particles, Mie requires more complex phase functions
P-N Approximation (Spherical Harmonics)	Expands radiation intensity as a series of spherical harmonics	Optical transport, planetary atmospheres	Higher orders improve accuracy	Computationally expensive for higher-order terms
Monte Carlo Method	Simulates photon trajectories stochastically	Remote sensing, biomedical optics, astrophysics	Very accurate, handles complex geometries	Computationally expensive, slow for large simulations
Beer's Law Approximation	Assumes exponential attenuation of direct radiation	Optical filters, thin clouds, atmospheric transmittance	Simple and fast, widely used	Ignores multiple scattering, only valid for direct light
k-Distribution Method	Reorders absorption coefficients by probability distribution	Climate models, gas absorption calculations	More accurate than band averaging, improves spectral resolution	Requires precomputed spectral data
Eddington Approximation (2-Stream Eddington Method)	Assumes isotropic intensity in forward and backward directions and linear angular dependence	Radiative transfer in atmospheres, cloud modeling	Improves accuracy over basic 2-stream	Less accurate for highly anisotropic scattering
Planck Mean Approximation	Averages absorption coefficient using a blackbody weighting function	Combustion modeling, atmospheric gas absorption	Simplifies spectral integration, useful for gas-phase radiative transfer	Less accurate in nonlocal thermodynamic equilibrium conditions, ignores spectral variations
Rosseland Mean Approximation	Uses Rosseland mean opacity, averaging absorption over spectrum	Astrophysical plasmas, high-energy radiation transport	Converts RTE into a simple diffusion equation, reducing computation	Fails in optically thin media, assumes local thermodynamic equilibrium

In general photometry, RTE remains the most comprehensive and challenging equation because of its integro-differential nature and multi-dimensional solutions, depending on the angular distribution and counting three interactions, each varying with wavelength and direction.

5. Actinic Effects of Light

Actinic flux measurement is not new in photometry; it has been studied since the early 20th century related to photobiology. The initial approach was on the biological effects of UV radiation on living organisms, thus laying the foundations of actinometry [61]. It has been proven that optical radiation has a critical role not only in human vision, but also in various photobiological and photochemical processes. These radiation-induced changes in both living and nonliving systems are known as *actinism* or actinic phenomena and an action spectrum is defined as the relative spectral effectiveness of optical radiation for a specified actinic phenomenon, in a specified system [23]. Following the need for metrological approaches towards standardizing these measurements to obtain reliable quantitative information, BIPM [62] defined photochemical or photobiological quantities in purely physical terms as a value derived from the corresponding radiometric quantity, assessed based on its effect on a selective receptor. Similarly to photometric quantities, it is determined by integrating the spectral distribution of the radiometric quantity over wavelength, weighted by the relevant actinic spectrum. Integration inherently assumes an arithmetic additivity law for photochemical or photobiological quantities, though real-world effects may not always follow this perfectly. Same as the action spectra for vision (Figure 4), the action spectrum for other actinic effects is a relative measure, typically normalized to one at the wavelength where the effect is most pronounced [63]. Thus, the weighting function is a relative, dimensionless quantity with an SI unit of one and the radiant quantity has the radiometric unit corresponding to that quantity.

If an effect is purely actinic—meaning it involves only chemical or molecular interactions—its magnitude depends on the number of absorbed photons. Consequently, the weighting function in the spectral photon system $s_p(\lambda)$ is proportional to the absorption spectrum of the actinic material, requiring a conversion before it can be used in the spectral power distribution system:

$$s_p(\lambda) = s_e(\lambda) / (h \cdot c / \lambda) \quad (20)$$

where $s_e(\lambda)$ is the weighting function in the spectral radiometric system and $\frac{hc}{\lambda}$ is the energy of a single photon at wavelength λ .

Conversely, if an effect is purely thermal—resulting from heating without chemical change and thus dependent on the absorbed energy—the weighting function in the spectral radiometric system is proportional to the absorption spectrum. Also, a conversion is necessary to adapt the absorption spectrum for use in the spectral photon system.

For a general response process, X , the relation between the two spectral weighting functions $s_{p,X}(\lambda)$ and $s_{e,X}(\lambda)$ describe the same effect as follows:

$$s_{p,X}(\lambda) = \gamma_X \times [(h \cdot c) / (\lambda \cdot n_a(\lambda))] \times s_{e,X}(\lambda) \quad (21)$$

where $\gamma_X [J^{-1}]$ is a constant, independent of the spectral irradiance, satisfying the requirement to set the maximum values of $s_{p,X}(\lambda)$ to 1, and n_a is the refractive index in air at specific wavelength λ . $s_{p,X}(\lambda)$ and $s_{e,X}(\lambda)$ have different forms and the peak wavelength of the effect is different when expressed in photon quantities or radiometric quantities [64].

For actinic effects in general, the generalized equation for the effect of light on a system would be

$$effect = \int s(\lambda) \cdot \phi(\lambda) d\lambda \quad (22)$$

And the effective exposure of human to radiation would be

$$H_{eff} = \int_{\lambda_1}^{\lambda_2} H_\lambda s(\lambda) d\lambda \quad (23)$$

As optical penetration into tissue is superficial, a surface exposure dose is most generally in the context of the CIE dose H_{eff} . The spectral characteristics of the exposure are quantified by quantities as the spectral irradiance or spectral radiant exposure H_λ [65] and the actinic weighting function $s(\lambda)$ depend on the biological effect, e.g., erythral response, DNA damage, or circadian response.

From these foundations of actinism emerged the concept of human centric lighting or integrative lighting. It refers to physiological and psychological effects of visible radiation on the human body, addressing both photobiological and photochemical processes. There are, by now, four known major reactions of the human body to incident light radiation: vision, circadian rhythm, regulation of mood and cognitive function, and skin damage under UV component. Along with Equation (23), broadly applicable to photobiological effects, there are other general equation used for modeling and quantifying the actinic response:

- To assess the effectiveness of lighting on circadian regulation, the melanopic equivalent daylight illuminance (M-EDI) has to be calculated:

$$E_{v, \text{mel}} = \sum_{\lambda} E_{\lambda} V_{\lambda}^{\text{mel}} \Delta \lambda \quad (24)$$

V_{λ}^{mel} is the melanopic spectral sensitivity function (dimensionless, normalized to 1 at 480 nm) [66].

- To assess how light affects sleep–wake cycles and overall circadian health, the circadian stimulus (CS) model has to be applied:

$$CS = 0.7 - \frac{0.7}{1 + \left(\frac{E_{v, \text{mel}} \times t \times f}{355.7} \right)^{1.1026}} \quad (25)$$

where t is the exposure time in hours, f is a factor for three different viewing modes, with values: 2 for a full visual field, 1 for a central visual field, and 0.5 for a superior visual field [67].

- To assess the spectral composition of a light source relative to daylight (widely used in human-centric lighting design), melanopic daylight efficacy ratio has to be calculated:

$$M_{\text{DER}} = \frac{M_{\text{EDI}}}{E_v} \quad (26)$$

- To assess the impact of light on the circadian system based on the spectral composition of the light source, melanopic ratio has to be determined:

$$MR = \frac{\text{Melanopic content}}{\text{Photopic content}} \cdot 1.218 \quad (27)$$

MR can be multiplied by a specified illuminance to determine equivalent melanopic lux, which is not an SI unit and has no standardized interpretation [68], but is more comprehensible when quantifying the effect of interior lighting to humans.

Since 2014, CIE regulated both visual performance and non-visual biological effects, through several publications: CIE 213:2014—Guide to protocols for lighting, color and vision research; CIE TN 003:2015—Report on the first international workshop on circadian and neurophysiological photometry; CIE 227:2017—Lighting for older people and people with visual impairments in buildings; CIE S 026/E:2018—System for metrology of optical radiation for ipRGC-influenced responses to light; and CIE Position Statement on Non-Visual Effects of Light:2019—Recommending proper light at the proper time. Also,

the International Organization for Standardization (ISO) and the International Electrotechnical Commission (IEC) have developed several standards pertinent to human-centric lighting: [69] for integrative lighting and non-visual effects, [70] for fluorescent lamps performance, [71] for compact fluorescent lamps used in general lighting and [72] for LED lighting safety specifications.

Actinic flux and irradiance related to human response can be measured with specific instrumentation, such as spectroradiometers, actinometers, melanopic sensors, UV radiometers, luxmeters with actinic filters, radiometers with actinic sensitivity, and hyperspectral imaging sensors. Each instrument is designed to operate in different applications but must consider jointly some factors to ensure reliable actinic flux measurements: they must be calibrated with the appropriate spectral sensitivity curves, must cover the relevant wavelength range for the effect being studied, must provide high precision measurements, and must operate regardless of environmental variations in temperature or humidity.

Furthermore, actinic flux measurement is conducted in other different fields, such as environmental monitoring (through ground-based networks or satellite observations), climate studies, and photochemical reaction modeling [73]. The recently developed instrumentation (miniaturized spectroradiometers which capture total hemispheric radiation from all angles, hyperspectral sensors, drones, high-altitude pseudo-satellites (HAPS)) provides input data with high accuracy and resolution for AI models. For instance, miniaturized hyperspectral cameras integrated with drones enables the collection of high-resolution spectral data, which can be processed using AI algorithms to classify materials and detect specific conditions in real-time [74]. Additionally, the fusion of multispectral imagery and spectrometer data from unmanned aerial vehicles (UAVs) has been explored to simulate hyperspectral image data, providing a cost-effective approach for precision farming applications [75].

6. Lighting Audit

A comprehensive evaluation of a lighting system is given by lighting audit. Its main objective is to identify measures to improve energy efficiency and to ensure optimal lighting. To completely fulfill its aims, audits must be expanded beyond quantitative energy and lighting optimization and include qualitative lighting assessment and human-centric metrics. Basically, it evaluates illuminance levels, spectral composition, glare, and light distribution to ensure compliance with visual comfort and efficiency standards; however, of the same importance, M-EDI should at least be mandatory. For public buildings, audit recommendations should target personalized and adaptive lighting, as human-centric lighting requires dynamic controls, sensors, and AI-driven lighting management to optimize exposure throughout the day (e.g., tunable white LED systems, occupancy-based dimming, daylight usage). It is possible for these two main goals (energy and lighting efficiency and human centric lighting) to contravene each other, if a system must simultaneously reduce luminaire consumption and provide circadian efficiency. In this case, a more complex audit should be conducted, to calculate MR specific to the occupancy and activity within the building [76], whose values can be achieved by varying the correlated color temperature (CCT) at the same light output, and CS index, whose values can be achieved by varying the light output, maintaining the same correlated color temperature [77]. A balanced approach should be adopted according to the specific activity (e.g., for office buildings $MR > 0.65$ and $CS > 0.3$, for medical buildings $MR > 0.8$ and $CS > 0.4$), and final audit recommendations must integrate dynamic CCT tuning and smart lighting automation for circadian-adaptive dimming profiles.

Lighting audits are not uniformly regulated across all countries: the United States adopted various standards and guidelines to support conducting lighting audits in build-

ings (ASHRAE 90.1, International Energy Conservation Code, Occupational Safety and Health Administration requirements, Illuminating Engineering Society standards RP-1 and RP-6 [78]), and the European Union started to implement directives as the Ecodesign Directive set requirements for energy-related products, including lighting; but they are not uniformly yet applied.

7. Conclusions

Lighting measurement and calculations have significantly evolved to address both visual and non-visual effects of light, reflecting the growing recognition of light's biological and physiological influence. Modern photometry now integrates principles from radiometry, quantum measurement, and photobiology to provide a more comprehensive understanding of luminous environments. This expanded scope requires not only precise instrumentation—accounting for factors such as spectral mismatch and calibration standards—but also advanced metrics that consider circadian and actinic effects.

The incorporation of spectral weighting functions and human-centric evaluation criteria enables lighting designs that go beyond efficiency, supporting visual comfort, biological rhythms, and overall well-being. As technologies such as hyperspectral sensors and AI-enhanced analytics continue to advance, lighting assessments are expected to become more targeted and adaptive.

Comprehensive lighting audits, grounded in established standards from organizations like CIE, ISO, and IEC, offer a framework for evaluating both quantitative and qualitative lighting parameters. These audits are instrumental in aligning lighting systems with performance, health, and regulatory goals, particularly in workplaces, healthcare, and residential settings. Overall, the integration of traditional and emerging methodologies marks a critical shift toward more holistic and human-centered lighting practices.

Author Contributions: Conceptualization, E.S., C.D. and M.C.T.; investigation, E.S. and C.D.; resources, E.S.; data curation, E.S.; writing—original draft preparation, E.S., C.D. and M.C.T.; writing—review and editing, E.S.; supervision, C.D. All authors have read and agreed to the published version of the manuscript.

Funding: This review draws upon foundational research conducted within the framework of the project “Real-time irrigation control and monitoring system, to optimize energy and water consumption”, SMIS code 338187, founded by North East Regional Program 2021–2027, PR/NE/2024/P1/RSO1.1_RSO1.3/1.

Data Availability Statement: The data are available on request from the corresponding author [E.S.].

Conflicts of Interest: The authors declare no conflicts of interest.

References

1. Chitu, C.; Dumitran, A.; Manole, C.; Antohe, S. The Light—an integrated approach to the phenomenon. *Procedia-Soc. Behav. Sci.* **2011**, *15*, 277–283. [\[CrossRef\]](#)
2. Khan, S.A. Medieval Arab contributions to optics. *Dig. Middle East Stud.* **2016**, *25*, 19–35. [\[CrossRef\]](#)
3. Dijksterhuis, F.J. Conjunctions in Paris: Interactions Between Rømer and Huygens. *Centaurus* **2012**, *54*, 58–76. [\[CrossRef\]](#)
4. Aldersey-Williams, H. *Dutch Light: Christiaan Huygens and the Making of Science in Europe*; Pan Macmillan: London, UK, 2020.
5. Klem-Musatov, K.; Hoeber, H.C.; Moser, T.J.; Pelissier, M.A. *Classical and Modern Diffraction Theory*; Society of Exploration Geophysicists: Tulsa, OK, USA, 2016; Volume 29, Chapter 1; p. 117.
6. Birch, T. Hypothesis Explaining the Properties of Light. In *The History of the Royal Society*; A. Millar: London, UK, 1757; Volume 3, pp. 247–305.
7. Gage, J. *Kulturgeschichte der Farbe: Von der Antike bis zur Gegenwart*; Moses, M., Opstelten, B., Trans., Eds.; Ravensburger Buchverlag: Ravensburg, Germany, 1994.
8. Wong, S.G. The composition of light in Newton's Opticks. *Prose Stud.* **1993**, *16*, 119–147. [\[CrossRef\]](#)
9. Lipson, A.; Lipson, S.G.; Lipson, H. *Optical Physics*; Cambridge University Press: Cambridge, UK, 2010.

10. Engheta, N. 150 years of Maxwell's equations. *Science* **2015**, *349*, 136–137. [CrossRef]
11. Mochrie, S.; De Grandi, C. Maxwell's Equations and Then There Was Light. In *Introductory Physics for the Life Sciences*; Springer: Cham, Switzerland, 2023.
12. Sarkar, T.K.; Dyab, W.; Palma, M.S. What did Maxwell do to prove light was electromagnetic in nature and the concept of his displacement current. In Proceedings of the 2012 IEEE International Conference on Wireless Information Technology and Systems (ICWITS), Maui, HI, USA, 11–16 November 2012; pp. 1–4.
13. Milonni, P.W.; Boyd, R.W. Momentum of light in a dielectric medium. *Adv. Opt. Photonics* **2010**, *2*, 519–553. [CrossRef]
14. Chiatti, L. On Some Forgotten Formulas of L. de Broglie and the Nature of Thermal Time. *Entropy* **2024**, *26*, 692. [CrossRef]
15. Elbaz, C. Wave-particle duality in Einstein-de Broglie programs. *J. Mod. Phys.* **2014**, *5*, 2192–2199. [CrossRef]
16. Drezet, A. Whence Nonlocality? Removing Spooky Action-at-a-Distance from the de Broglie Bohm Pilot-Wave Theory Using a Time-Symmetric Version of the de Broglie Double Solution. *Symmetry* **2024**, *16*, 8. [CrossRef]
17. Bertenshaw, D.R. *Light and Photometry, the Path to Standardisation*; Die Vierte Wand; Initiative TheaterMuseum Berlin e.V.: Berlin, Germany, May 2019; Volume 009, pp. 152–163.
18. Palaz, A. *A Treatise on Industrial Photometry with Special Application to Electric Lighting*, 2nd ed.; Patterson, G.W., Trans., D., Eds.; Van Nostrand Company: London, UK, 1896.
19. Raju, M.P.; T'ien, J.S. Modelling of candle burning with a self-trimmed wick. *Combust. Theory Model.* **2008**, *12*, 367–388. [CrossRef]
20. Paterson, C.C. XXXIV. The proposed international unit of candle power. *Lond. Edinb. Dublin Philos. Mag. J. Sci.* **1909**, *18*, 263–274. [CrossRef]
21. Saha, S.; Jaiswal, V.K.; Sharma, P.; Aswal, D.K. Evolution of SI base unit candela: Quantifying the light perception of human eye. *Mapan* **2020**, *35*, 563–573. [CrossRef]
22. Higgs, P. Candle-power of the electric light. *Minutes Proc. Inst. Civ. Eng.* **1882**, *68*, 117–122. [CrossRef]
23. Zwinkels, J.C.; Ikonen, E.; Fox, N.P.; Ulm, G.; Rastello, M.L. Photometry, radiometry and 'the candela': Evolution in the classical and quantum world. *Metrologia* **2010**, *47*, R15. [CrossRef]
24. Zong, Y. From candle to candela. *Nat. Phys.* **2016**, *12*, 614. [CrossRef]
25. Sperling, A.; Kück, S. The SI Unit Candela. *Ann. Der Phys.* **2019**, *531*, 1800305. [CrossRef]
26. Islam, M.R.; Ali, M.M.; Lai, M.-H.; Lim, K.-S.; Ahmad, H. Chronology of Fabry-Perot Interferometer Fiber-Optic Sensors and Their Applications: A Review. *Sensors* **2014**, *14*, 7451–7488. [CrossRef]
27. Wei, C.; Li, L. Ultrasonic/Acoustic Methods for Process Monitoring. In *Handbook of Laser Micro- and Nano-Engineering*; Sugioka, K., Ed.; Springer Nature Switzerland AG: Cham, Switzerland, 2020; p. 12.
28. González-García, A.; Pottiez, O.; Grajales-Coutiño, R.; Ibarra-Escamilla, B.; Kuzin, E.A. Optical pulse compression and amplitude noise reduction using a non-linear optical loop mirror including a distributed Gires-Tournois etalon. *Opt. Laser Technol.* **2010**, *42*, 1103–1111. [CrossRef]
29. Amiel, Y.; Nedvedski, R.; Mandelbaum, Y.; Tischler, Y.R.; Tischler, H. Super-Spectral-Resolution Raman spectroscopy using angle-tuning of a Fabry-Pérot etalon with application to diamond characterization. *Spectrochim. Acta Part A Mol. Biomol. Spectrosc.* **2025**, *325*, 125038. [CrossRef]
30. Gu, S.; Hou, X.; Li, N.; Yi, W.; Ding, Z.; Chen, J.; Hu, G.; Dou, X. First comparative analysis of the simultaneous horizontal wind observations by collocated meteor radar and FPI at low latitude through 892.0-nm airglow emission. *Remote Sens.* **2021**, *13*, 4337. [CrossRef]
31. Bertenshaw, D.R. The standardisation of light and photometry—A historical review. *Light. Res. Technol.* **2020**, *52*, 816–848. [CrossRef]
32. Available online: <https://www.radiantvisionsystems.com/products/imaging-colorimeters-photometers/prometric-y-imaging-photometers> (accessed on 1 December 2024).
33. Available online: <https://labsphere.com/wp-content/uploads/2021/09/Integrating-Sphere-Radiometry-and-Photometry.pdf> (accessed on 2 December 2024).
34. Pavlov, D.; Ivanov, D. Methods to Improve Quantitative and Qualitative Indicators of Lighting in Classrooms. In Proceedings of the 2022 14th Electrical Engineering Faculty Conference (BuleF), Varna, Bulgaria, 14–17 September 2022; IEEE: New York, NY, USA, 2022; pp. 1–4.
35. Panahiazar, S.; Matkan, M. Qualitative and quantitative analysis of natural light in the dome of San Lorenzo, Turin. *Front. Arch. Res.* **2018**, *7*, 25–36. [CrossRef]
36. Tabaka, P.; Wtorkiewicz, J. Analysis of the Spectral Sensitivity of Luxmeters and Light Sensors of Smartphones in Terms of Their Influence on the Results of Illuminance Measurements—Example Cases. *Energies* **2022**, *15*, 5847. [CrossRef]
37. Wolfe, W. Spectrometers. In *Fundamentals and Basic Optical Instruments*; CRC Press: Boca Raton, FL, USA, 2017; pp. 405–446.
38. Meunier, B.; Cosmas, J.; Ali, K.; Jawad, N.; Eappen, G.; Zhang, X.; Zhao, H.; Li, W.; Zhang, H. Visible light positioning with lens compensation for non-Lambertian emission. *IEEE Trans. Broadcast.* **2023**, *69*, 289–302. [CrossRef]

39. Spieringhs, R.M.; Phung, T.H.; Audenaert, J.; Hanselaer, P. Exploring the Applicability of the Unified Glare Rating for an Outdoor Non-Uniform Residential Luminaire. *Sustainability* **2022**, *14*, 13199. [\[CrossRef\]](#)
40. Andrews, S.S. Color. In *Light and Waves: A Conceptual Exploration of Physics*; Springer International Publishing: Cham, Switzerland, 2023; pp. 249–271.
41. Dang, R.; Guo, W.; Luo, T. Correlated colour temperature index of lighting source for polychrome artworks in museums. *Build. Environ.* **2020**, *185*, 107287. [\[CrossRef\]](#)
42. Ren, Z.; Fang, F.; Yan, N.; Wu, Y. State of the art in defect detection based on machine vision. *Int. J. Precis. Eng. Manuf.-Green Technol.* **2022**, *9*, 661–691. [\[CrossRef\]](#)
43. Available online: <https://www.flusmeter.com/what-factors-affect-the-measurement-results-of-a-light-meter> (accessed on 7 October 2025).
44. ISO/IEC 17025:2017; General Requirements for the Competence of Testing and Calibration Laboratories. International Organization for Standardization: Geneva, Switzerland, 2017.
45. CIE 198-SP2:2018; Determination of Measurement Uncertainties in Photometry Supplement 2: Spectral measurements and derivative quantities. CIE: Vienna, Austria, 2018; ISBN 978-3-902842-11-4.
46. CIE TN 009:2019; The Use of “Accuracy” and Related Terms in the Specifications of Testing and Measurement Equipment, Technical Note. CIE: Vienna, Austria, 2019.
47. Castro, P.J.; Payne, T.; Frey, V.C.; Kinader, K.K.; Godar, T.J. Calculating photometric uncertainty. In Proceedings of the AMOS Technical Conference, Maui, HI, USA, 15–18 September 2020.
48. Song, W.; Durmus, D. Evaluating Energy Efficiency and Colorimetric Quality of Electric Light Sources Using Alternative Spectral Sensitivity Functions. *Buildings* **2022**, *12*, 2220. [\[CrossRef\]](#)
49. Lamb, T. Why rods and cones? *Eye* **2016**, *30*, 179–185. [\[CrossRef\]](#)
50. Ding, J.; Yao, Q.; Jiang, L. Comparisons of Scotopic/Photopic Ratios Using 2- and 10-Degree Spectral Sensitivity Curves. *Appl. Sci.* **2019**, *9*, 4471. [\[CrossRef\]](#)
51. Available online: <https://cie.co.at/datatable/cie-spectral-luminous-efficiency-photopic-vision> (accessed on 10 January 2024).
52. Available online: <https://cie.co.at/datatable/cie-spectral-luminous-efficiency-scotopic-vision> (accessed on 10 January 2024).
53. Jarosz, W.; Schönefeld, V.; Kobbelt, L.; Jensen, H.W. Theory, analysis and applications of 2D global illumination. *ACM Trans. Graph. (TOG)* **2012**, *31*, 1–21. [\[CrossRef\]](#)
54. Salguero-Andújar, F.; Cabeza-Lainez, J.-M. New Computational Geometry Methods Applied to Solve Complex Problems of Radiative Transfer. *Mathematics* **2020**, *8*, 2176. [\[CrossRef\]](#)
55. Zhang, Z.; Lou, C.; Kalayci, N.; Cai, W. Entropy and exergy analyses of a direct absorption solar collector: A detailed thermodynamic model. *Int. J. Heat Mass Transf.* **2025**, *239*, 126566. [\[CrossRef\]](#)
56. Wunsch, R. Radiation transport methods in star formation simulations. *Front. Astron. Space Sci.* **2024**, *11*, 1346812. [\[CrossRef\]](#)
57. Ramley, I.; Alzayed, H.M.; Al-Hadeethi, Y.; Chen, M.; Barasheed, A.Z. An Overview of Underwater Optical Wireless Communication Channel Simulations with a Focus on the Monte Carlo Method. *Mathematics* **2024**, *12*, 3904. [\[CrossRef\]](#)
58. Capilla, M.T.; Talavera, C.F.; Ginestar, D.; Verdú, G. A study of the radiative transfer equation using a spherical harmonics-nodal collocation method. *J. Quant. Spectrosc. Radiat. Transf.* **2017**, *189*, 25–36. [\[CrossRef\]](#)
59. Wei, J.; Shi, Y.; Ren, Y.; Li, Q.; Qiao, Z.; Cao, J.; Ayantobo, O.O.; Yin, J.; Wang, G. Application of Ground-Based Microwave Radiometer in Retrieving Meteorological Characteristics of Tibet Plateau. *Remote Sens.* **2021**, *13*, 2527. [\[CrossRef\]](#)
60. Lambert, J.; Paletou, F.; Josselin, E.; Glorian, J.M. Numerical radiative transfer with state-of-the-art iterative methods made easy. *Eur. J. Phys.* **2015**, *37*, 015603. [\[CrossRef\]](#)
61. Warburg, O. Über die Geschwindigkeit der photochemischen Kohlensäurezersetzung in lebenden Zellen. *Biochem. Z.* **1928**, *30*, 540–541.
62. BIPM. *The International System of Units (SI)*, 9th ed.; V3.01; BIPM: Sèvres, France, August 2024.
63. BIPM. *Principles Governing Photometry*, 2nd ed.; BIPM: Sèvres, France, 2019.
64. BIPM. *SI Brochure, 9th Edition (2019)—Appendix 3 v1.02, Units for Photochemical and Photobiological Quantities*; BIPM: Sèvres, France, 2021.
65. Sliney, D.H. Radiometric quantities and units used in photobiology and photochemistry: Recommendations of the Commission Internationale de l’Eclairage (International Commission on Illumination). *Photochem. Photobiol.* **2007**, *83*, 425–432. [\[CrossRef\]](#)
66. Noor, M.C.; Saradj, F.M.; Yazdanfar, S.A. Analytical evolution of measurement methods for light’s non-visual effects. *Results Eng.* **2023**, *17*, 100922. [\[CrossRef\]](#)
67. Huang, Y.; Li, J.; Dai, Q. Comparative analysis of circadian lighting models: Melanopic illuminance vs. circadian stimulus. *Opt. Express* **2024**, *32*, 29494–29513. [\[CrossRef\]](#)
68. Esposito, T.; Houser, K. Correlated color temperature is not a suitable proxy for the biological potency of light. *Sci. Rep.* **2022**, *12*, 20223. [\[CrossRef\]](#)

69. ISO/CIE TR 21783:2022 (First edition, 2022); Light and Lighting—Integrative Lighting—Non-visual Effects. ISO/CIE: Geneva, Switzerland, 2022.
70. IEC 60081:1997/AMD6:2017; Edition 5.0, Amendment 6. Double-capped Fluorescent Lamps—Performance Specifications. International Electrotechnical Commission: Geneva, Switzerland, 2017.
71. IEC 60969:2016; Edition 2.0. Self-ballasted Compact Fluorescent Lamps for General Lighting Services—Performance Requirements. International Electrotechnical Commission: Geneva, Switzerland, 2016.
72. IEC 62031:2018; Edition 2.0. LED Modules for General Lighting—Safety Specifications. International Electrotechnical Commission: Geneva, Switzerland, 2018.
73. Rabani, J.; Mamane, H.; Pousty, D.; Bolton, J.R. Practical chemical actinometry—A review. *Photochem. Photobiol.* **2021**, *97*, 873–902. [CrossRef] [PubMed]
74. Available online: <https://www.m4mining.eu/wp-content/uploads/2024/10/D3.1-UAS-integrated-with-multi-sensor-payload-ready-to-fly.pdf> (accessed on 7 February 2025).
75. Zeng, C.; King, D.J.; Richardson, M.; Shan, B. Fusion of Multispectral Imagery and Spectrometer Data in UAV Remote Sensing. *Remote Sens.* **2017**, *9*, 696. [CrossRef]
76. Available online: https://www.energy.gov/sites/prod/files/2020/03/f72/ssl-mp-ratios_lda_feb2020.pdf (accessed on 8 February 2025).
77. Kotsenos, A.; Madias, E.N.; Topalis, F.; Doulos, L. Circadian Stimulus Calculators as Environmental Building Design Tools: Early Results of a Critical Review. *IOP Conf. Ser. Earth Environ. Sci.* **2022**, *1123*, 012035. [CrossRef]
78. Available online: <https://www.starbeamlighting.com/lighting-regulations-and-compliance-for-commercial-buildings/> (accessed on 8 February 2025).

Disclaimer/Publisher’s Note: The statements, opinions and data contained in all publications are solely those of the individual author(s) and contributor(s) and not of MDPI and/or the editor(s). MDPI and/or the editor(s) disclaim responsibility for any injury to people or property resulting from any ideas, methods, instructions or products referred to in the content.